

Comparison of Resonant Frequency for Several Designs of SRR

Thill A. Kadhum Al-musawi^{1*}, Samira Adnan Mahdi², Sundus Yaseen Hasan AL-Asadi³

^{1*}Physics Department, Science College, Al-Muthanna University, Iraq

²Physics Department, Science College, Babylon University, Iraq

³Physics Department, Education College for Girls, Kufa University, Iraq

Corresponding Author: ^{1*}thillakeel@mu.edu.iq

Abstract: The area of this paper is to design and simulate the new structures having simultaneous negative permeability ϵ_{eff} and permittivity μ_{eff} , and index of refraction n_{eff} around (8- 12) GHz, the so-called left-handed material LHM. All designs have the same dimensions. The parameters of SRR have been varied such as split width, gap width, and metal width. Also, the negative values of ϵ_{eff} , μ_{eff} , and n_{eff} have been approved.

Keywords: Metamaterials, S- parameters, Split- ring resonator, Negative- index of refraction materials.

1. Introduction

A single cell SRR has a pair of opened rings with splits in them at cross ends. The rings are made of nonmagnetic metal as aluminum and have a gap between them. The rings can be concentric, or square, and gapped as needed, carved on dielectric substrates [1- 4]. A magnetic flux ingoing the rings will induce rotating currents in the rings, which produce their flux to increase or decrease the incident field. This type of field is dipolar. Due to splits in the rings of structure can support resonant wavelengths so larger than the rings diameter. This would not happen in unopened rings. SRR is applied to create negative values of μ , while the rod is applied to create negative values of ϵ [5- 9].

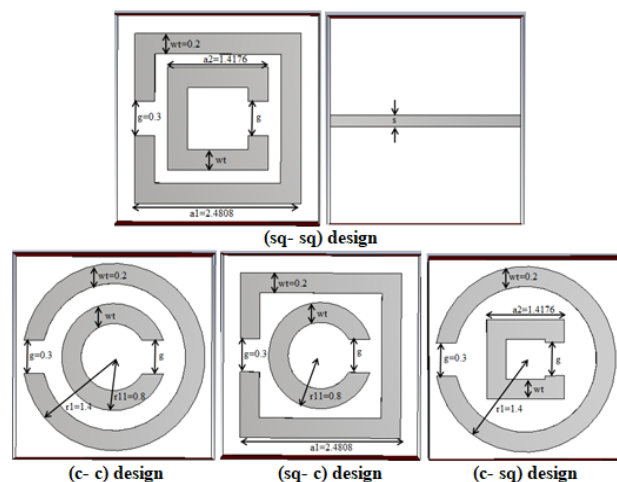


Figure 1. A typical unit cell of the left-handed structure contains SRR with a metallic rod placed on the dielectric board for square- square SRR (sq- sq design), circle- circle SRR (c- c design) square- circle SRR (sq- c design) and circle- square SRR (c- sq design).

2. Method

The parameters of the materials which appear in Maxwell's equations are the magnetic permeability μ and the dielectric permittivity ϵ [4, 5] it's the primary characteristic quantities that define the propagation of the electromagnetic waves in the matter. In this paper, the thin wire (rod) was used to get the negative permittivity, while the structure SRR was used to get the negative permeability, thus, the full structure (SRR-rod) was formed from the rod and the structure SRR which was used to get the negative refractive index [10-14].

3. Results and discussions

In this paper, different structures of the (SRR- rod) were presented, and the effect of these structures on resonant frequencies and other effective parameters like electric permittivity, magnetic permeability and refractive index were discussed by using simulated S-parameters in CST software. To study these effects, the structure parameters like split width, g , metal width, wt , and square side length, (a) were changed several times. Before studying these structure parameters, the effective frequency range must be specified as in the following section.

a. Effective frequency:

This design were performed a simulation was done with normal incidence and the magnetic field is polarized with y-axis while the electric field is polarized at x-axis to get S- parameters, with unit cell ($l=3$ mm), and the effective thickness of material sample is ($2.5 \mu\text{m}$). After the proper designs are completed, a simulation for frequency band (0- 30) GHz was run, and the results were drawn in figure 2. Form these figures, it can be concluded that the effective range of frequencies that contains the peaks and dips under interest is between (8- 16) GHz. and this range will be taken in the rest work in this paper.

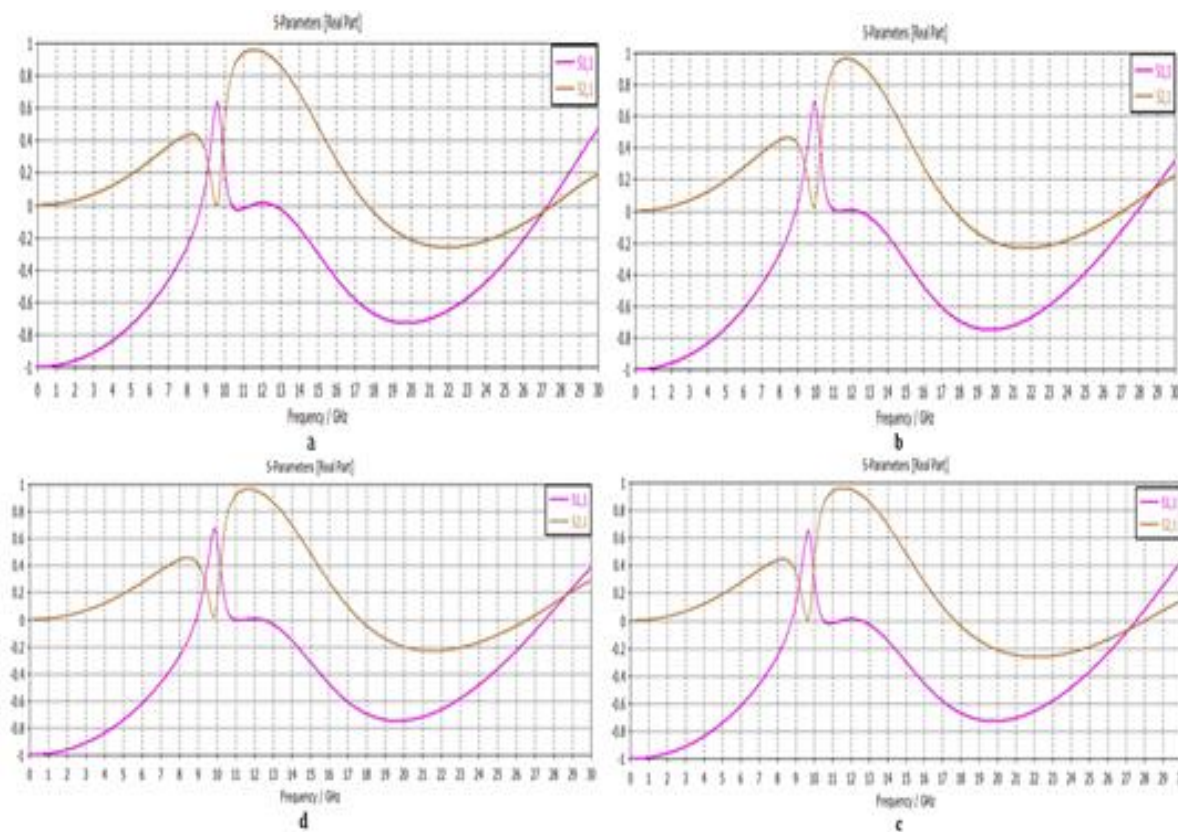


Figure 2. Real parts of S11 and S21 parameters with frequency band (0- 30) GHz for a) (sq- sq) design, b) (c- c) design, c) (sq- c) design, and d) (c- sq) design

b. Effects of changing design parameters

For the four designs, the parameters shown in figure 1 were discussed individually by keeping all other parameters constants as follows:

Effect of split width (g):

The split width was changed for the four designs as ($g=0.1- 0.5$) mm, while other parameters kept constants ($wt=0.2$, $s= 0.14$, $a1=2.480$ 8, $a2=1.4176$, $r1=1.4$ and $r2=0.8$) mm. Note that the area of outer circle of circular ring equal the area of the outer square of square ring, i.e. ($\pi r1^2=a1^2$ and $\pi r2^2=a2^2$). The real parts of S11 and S21 parameters were shown in figures (3- 6). From these figures, the effective resonance frequencies for all

designs have been found as in table 1, and it is obvious that the resonant frequency proportional directly with increasing gap distance for all four designs as in figure 4. This happens because of decreasing the capacitance that is proportional inversely with gap distance. By looking to figure 7 it can be concluded that the largest value of resonant frequency is for the design (c-c) and then (c-sq), (sq- c) and (sq- sq).

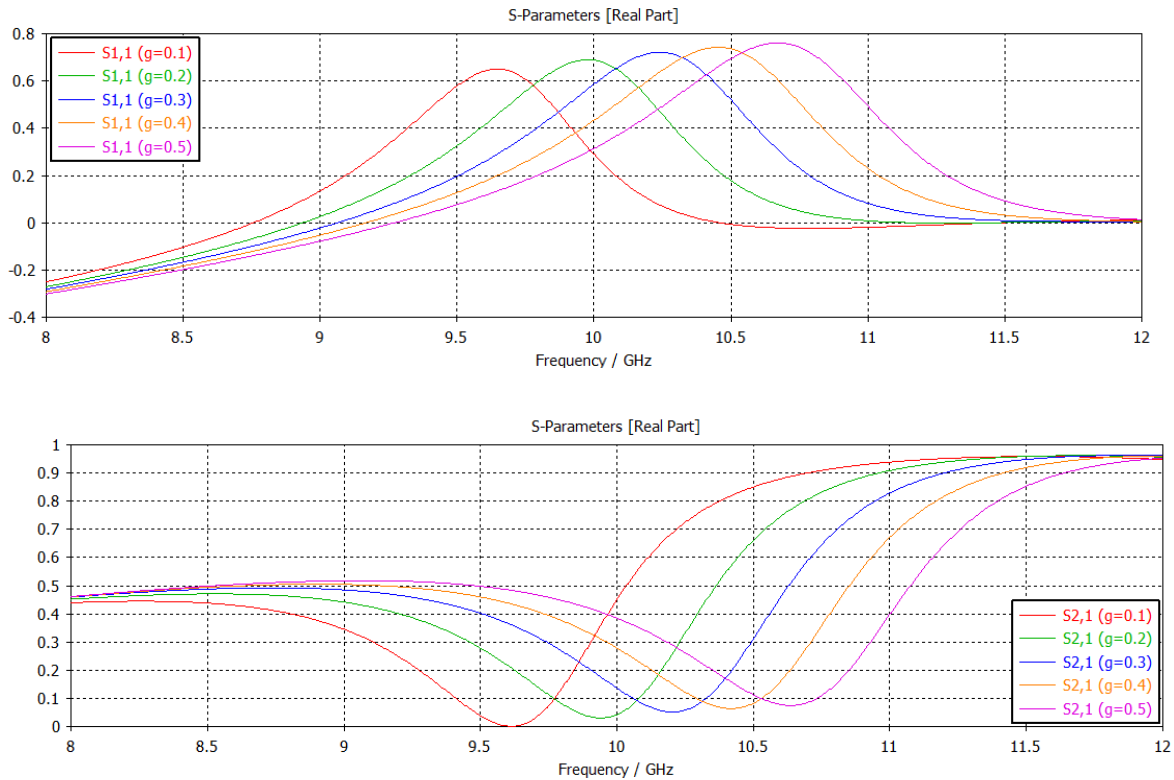
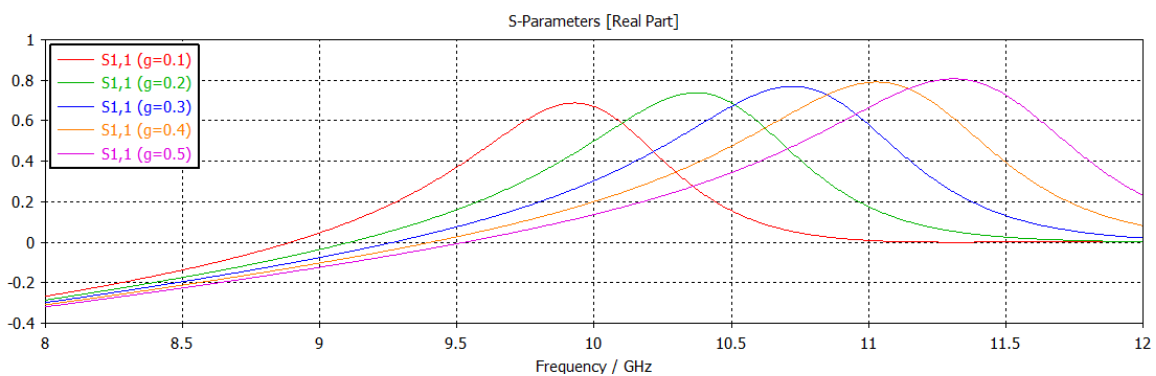


Figure 3. Real part of S₁₁ and S₂₁ parameters of SRR- rod for split width in (sq- sq) design.



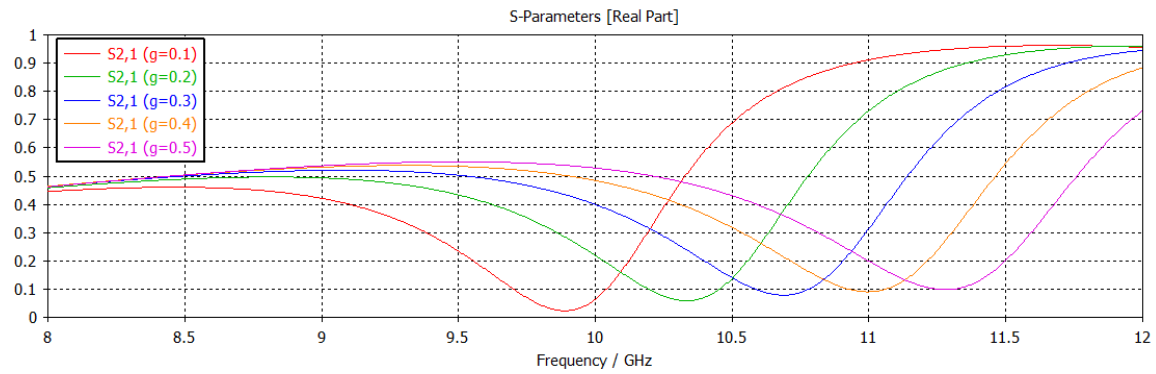


Figure 4. Real part of S11 and S21 parameters of SRR- rod for split width in (c- c) design.

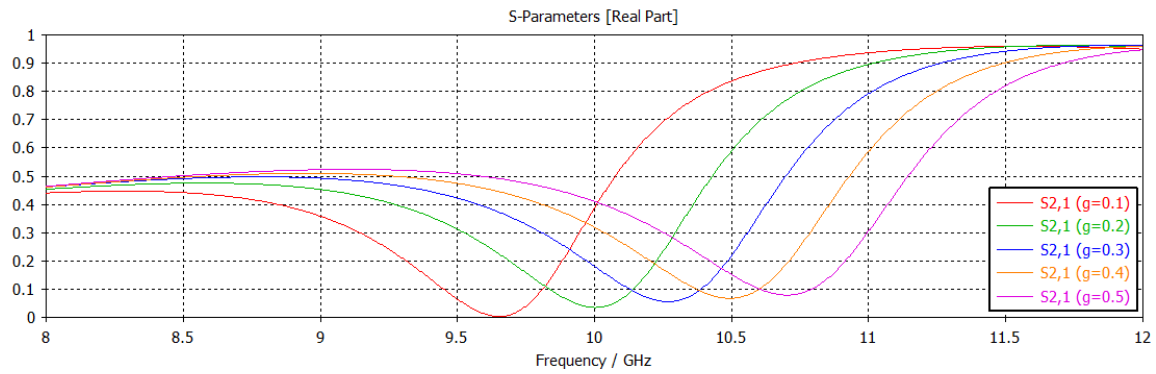
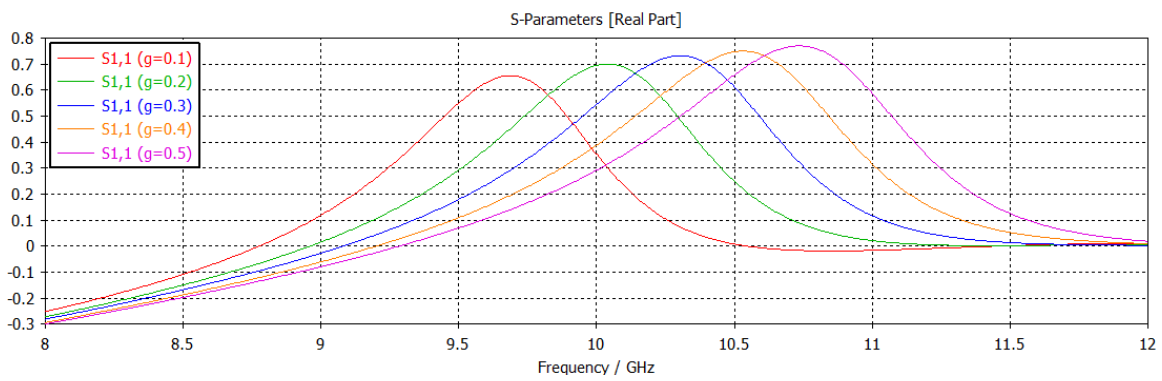
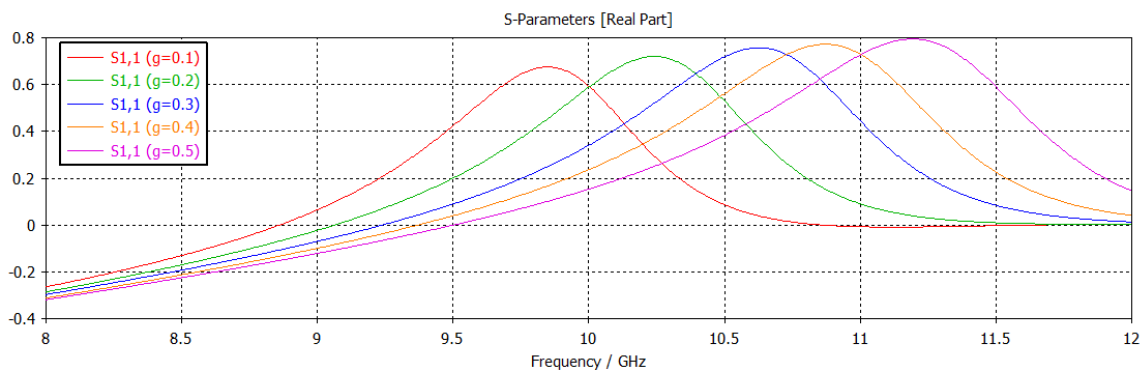


Figure 5. Real part of S11 and S21 parameters of SRR- rod for split width in (sq- c) design.



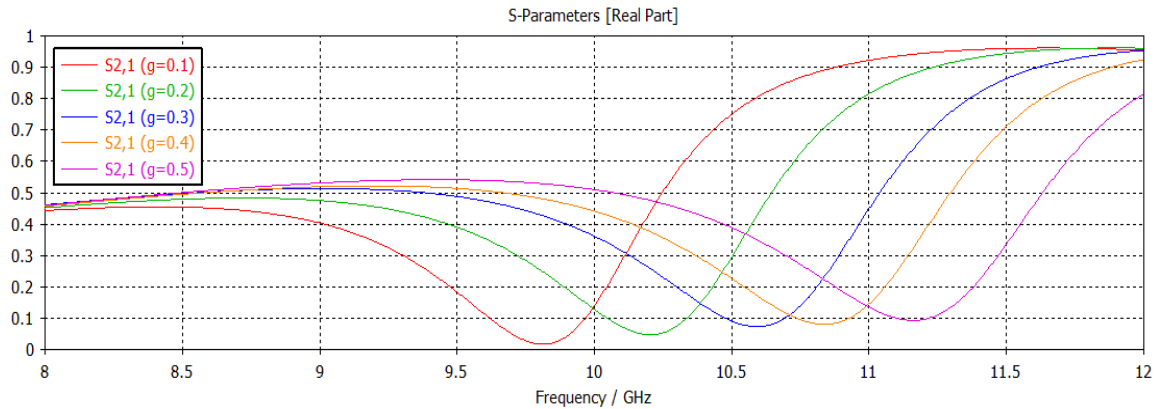


Figure 6. Real part of S11 and S21 parameters of SRR- rod for split width in (c- sq) design.

Table 1. Effective resonance frequency for every split width.

Split width g (mm)	Effective frequency f (GHz)							
	For sq- sq design		For c- c design		For sq- c design		For c- sq design	
	S11real	S21real	S11real	S21real	S11real	S21real	S11real	S21real
0.1	9.648	9.612	9.928	9.888	9.688	9.652	9.848	9.812
0.2	9.976	9.94	10.372	10.332	10.04	10.004	10.24	10.204
0.3	10.24	10.204	10.724	10.688	10.304	10.268	10.6	10.57
0.4	10.452	10.42	11.028	10.996	10.528	10.492	10.9	10.86
0.5	10.672	10.636	11.312	11.28	10.736	10.704	11.192	11.16

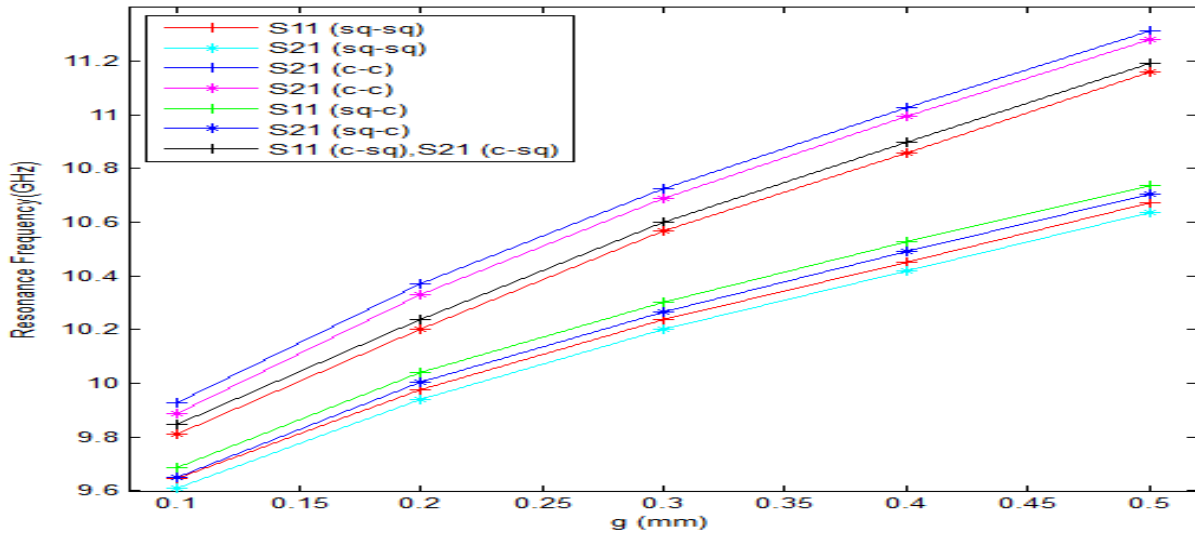


Figure 7. The values of resonance frequency versus gap distance g

To understand the influence on ϵ and μ , figure 8 shows the real parts for these parameters for (sq-sq) design. The real part of ϵ_{eff} is negative in range (8- 12) GHz while the real part of μ_{eff} is negative in range of frequency about (9.5- 12) GHz. That is, $\epsilon_{eff} < 0$ and $\mu_{eff} < 0$ are nearly in same frequency range which lead to get negative values of refractive index as in figure 9, and n_{eff} exhibits a negative values in the range (8- 12.8) GHz.

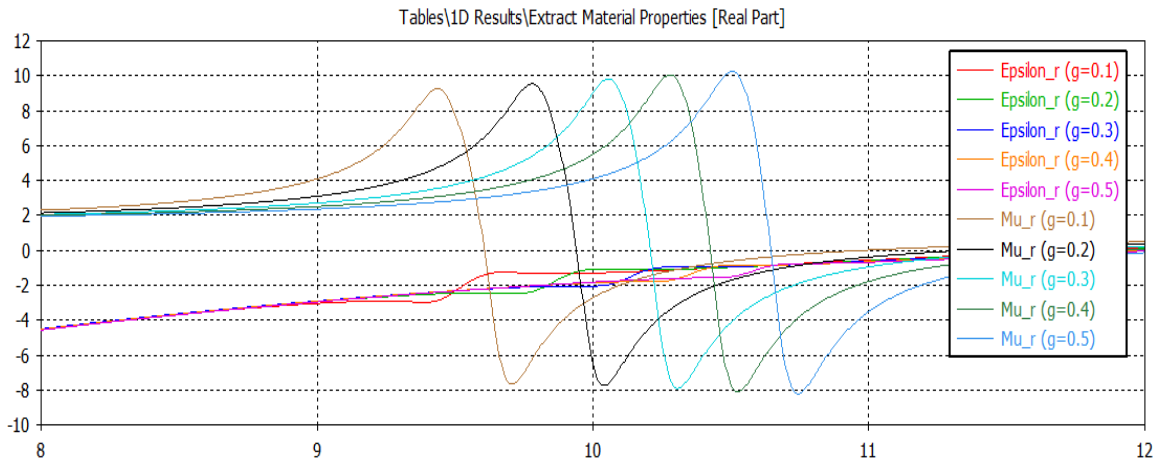


Figure 8. Real parts of electric permittivity ϵ and magnetic permeability μ for different split widths as in (sq- sq) design

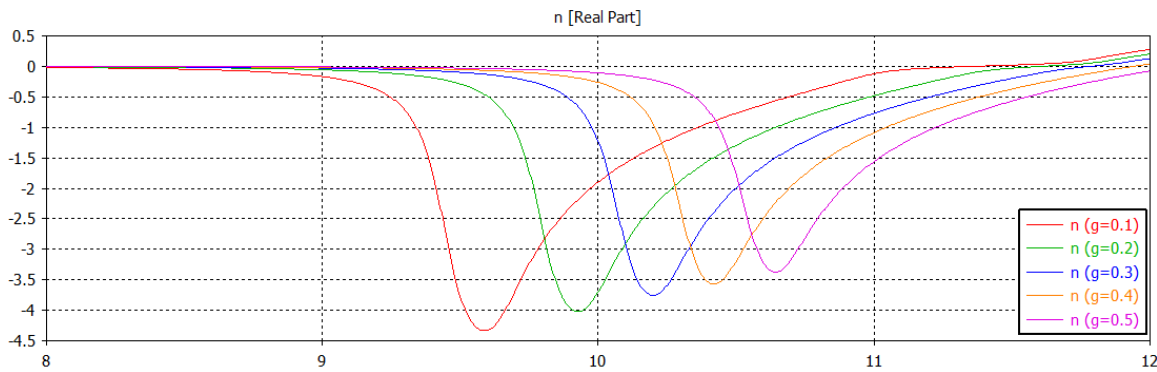
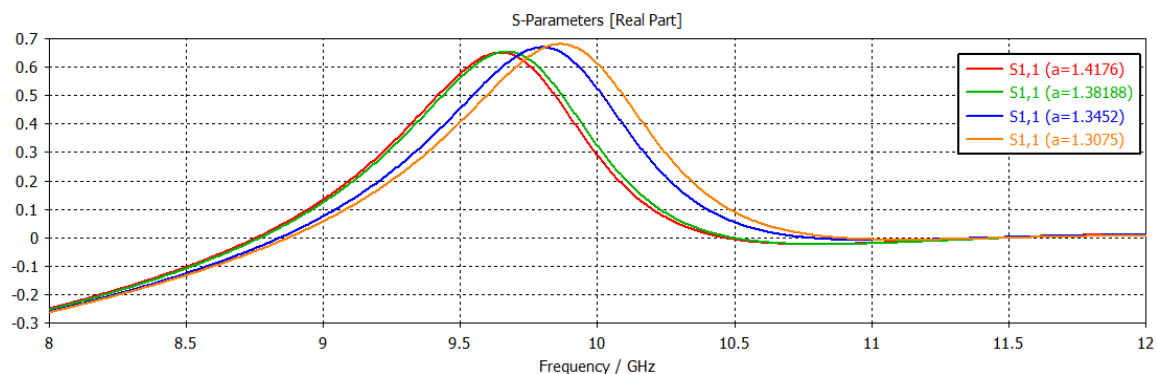


Figure 9. Real part of refractive index n for different split widths as in (sq- sq) design

i.Effect of changing the area between the rings (d):

In this section, the area between the outer and the inner rings were changed several times by changing the area of the inner ring. For the (sq- sq) and (c- sq) designs the area of the inner square has been changed by changing the length of its four sides (a_2), while for the (c- c) and (sq- c) designs the inner circle has been changed by changing the radius r_{11} . Also the other parameters are kept constants ($g= 0.1$, $wt= 0.2$, $s= 0.14$, $a_1=2.4808$, and $r_1=1.4$) mm.



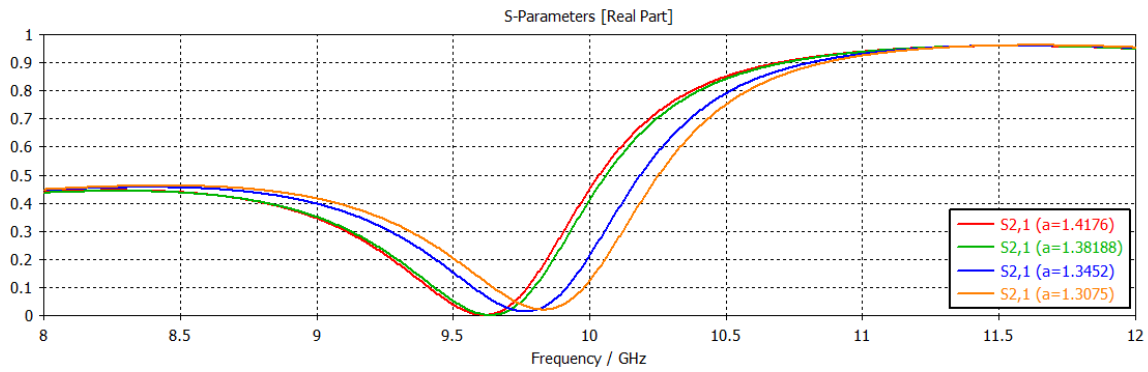


Figure 10. Real part of S11 and S21 parameters for different area between two the rings d as in (sq- sq) design.

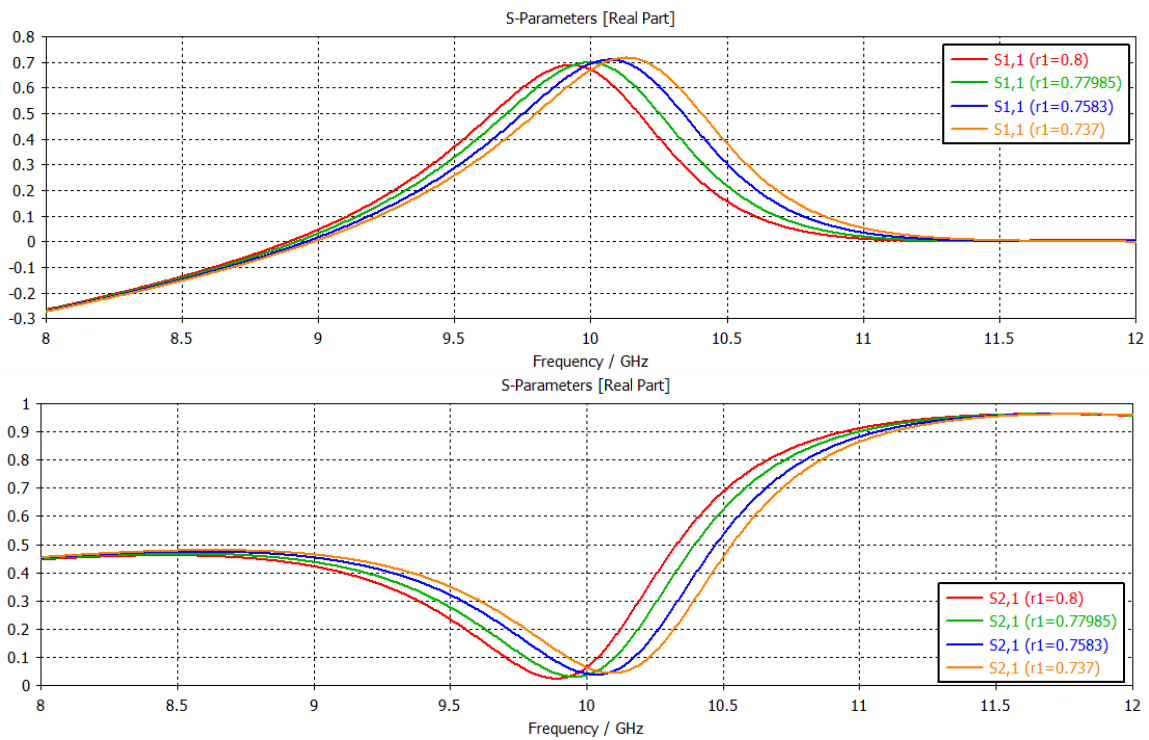
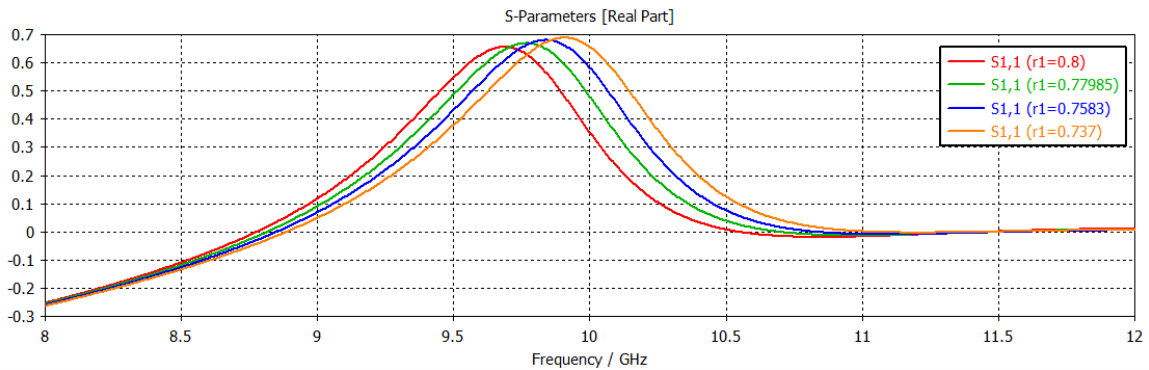


Figure 11. Real part of S11 and S21 parameters for different area between two the rings d as in (c- c) design.



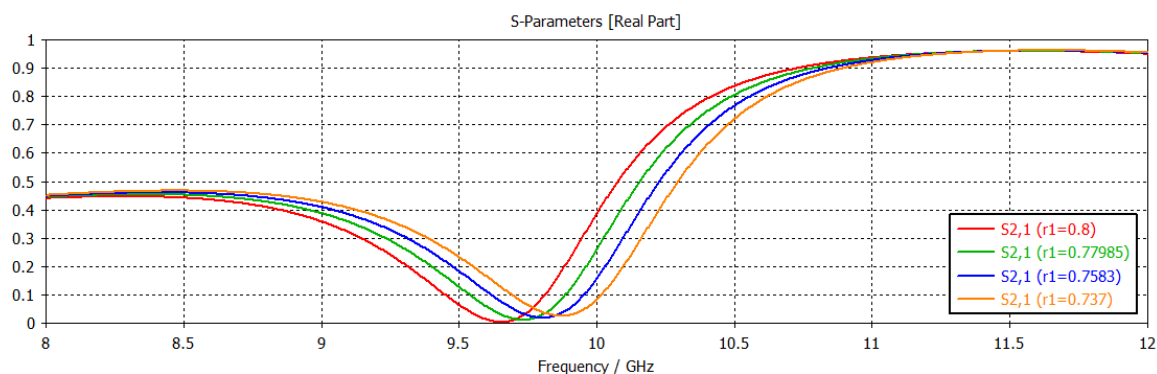


Figure12. Real part of S11 and S21 parameters for different area between two the rings d as in (sq- c) design.

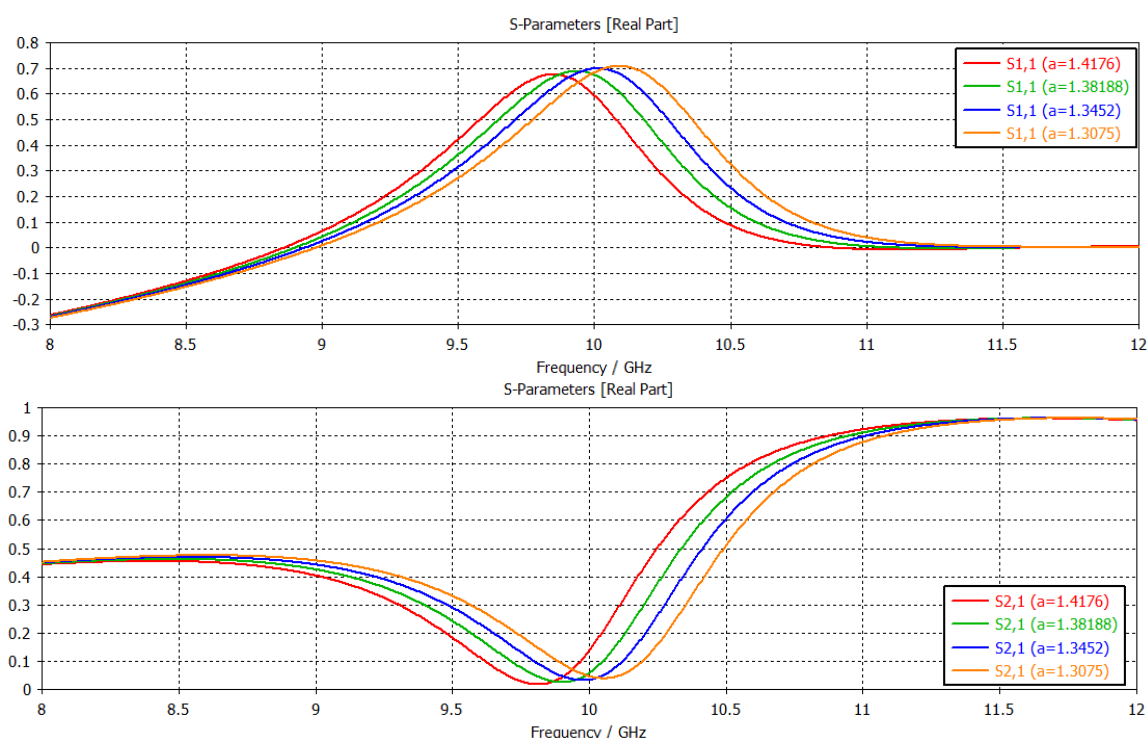


Figure 13. Real part of S11 and S21 parameters for different area between two the rings d as in (c- sq) design.

When (a2) and (r11) decrease the area between the rings is increase and this means the distance between the rings increase. This leads to a decrease in the self- inductance of the inner square and also there is a decrease in mutual capacitance and mutual inductance of the system. So, this will lead to an increase in ω_m , as illustrated in table 2 and Figure 14.

Table 2. Effective frequency for different values of distance between two the rings d.

Area between two the rings d (mm)	Effective frequency f (GHz)							
	For sq- sq design		For c- c design		For sq- c design		For c- sq design	
	S11real	S21real	S11real	S21real	S11real	S21real	S11real	S21real
3.19	9.628	9.622	9.928	9.92	9.688	9.672	9.848	9.832
3.29	9.7	9.69	9.992	9.98	9.768	9.752	9.936	9.927
3.39	9.77	9.76	10.072	10.062	9.836	9.82	10.012	10
3.49	9.834	9.826	10.128	10.12	9.908	9.89	10.092	10.082

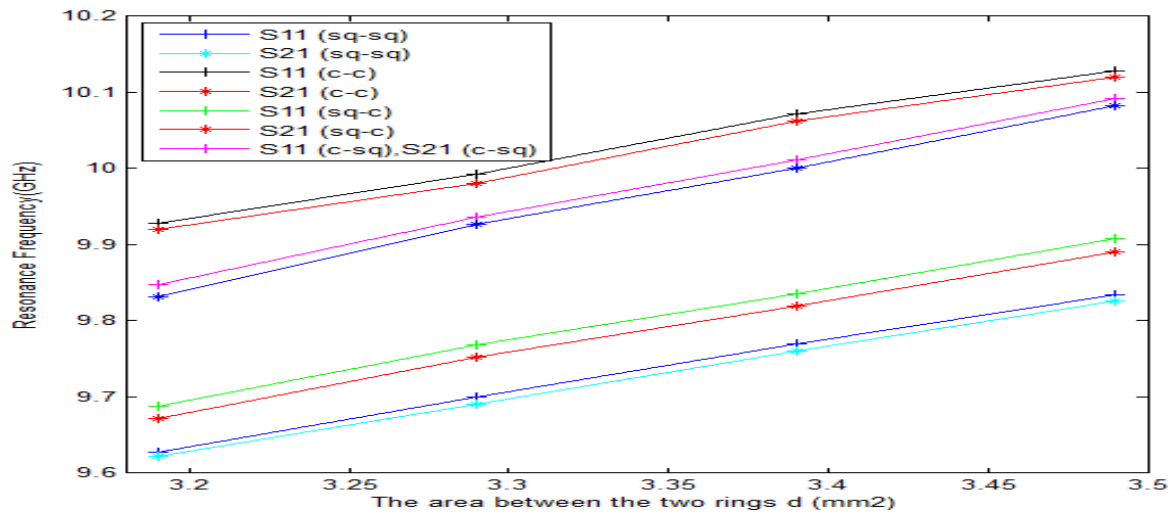


Figure 14. The values of resonance frequency versus area between two the rings d

By looking to figure 14 it can be concluded that the largest value of resonant frequency is for the design (c-c) and then (c-sq), (sq-c) and (sq-sq). These differences between the four designs were due to the difference in the space area between the two rings in four designs, since the circular area is larger than the square area, so the capacitance of circle is larger, and this gives a difference in the mutual capacitance and inductance between them. So resonant frequency is small due to the large of mutual capacitance.

The ϵ_{eff} and μ_{eff} for each design were calculated from S11 and S21, where $\epsilon_{eff} < 0$ and $\mu_{eff} < 0$ are simultaneously about (9.8- 12) GHz, as in figure 15, so n_{eff} is negative values around the limited frequencies as in figure 16.

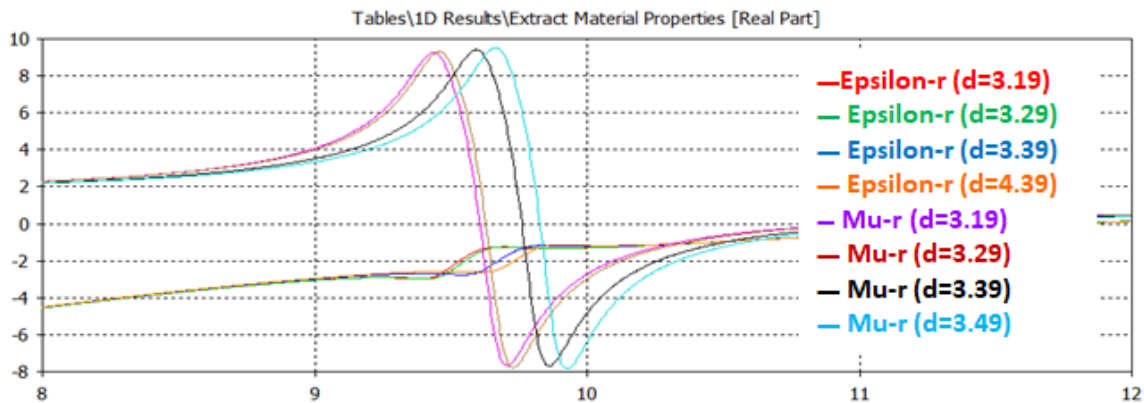


Figure 15. Real parts of electric permittivity ϵ and magnetic permeability μ for different split widths as in (sq-sq) design

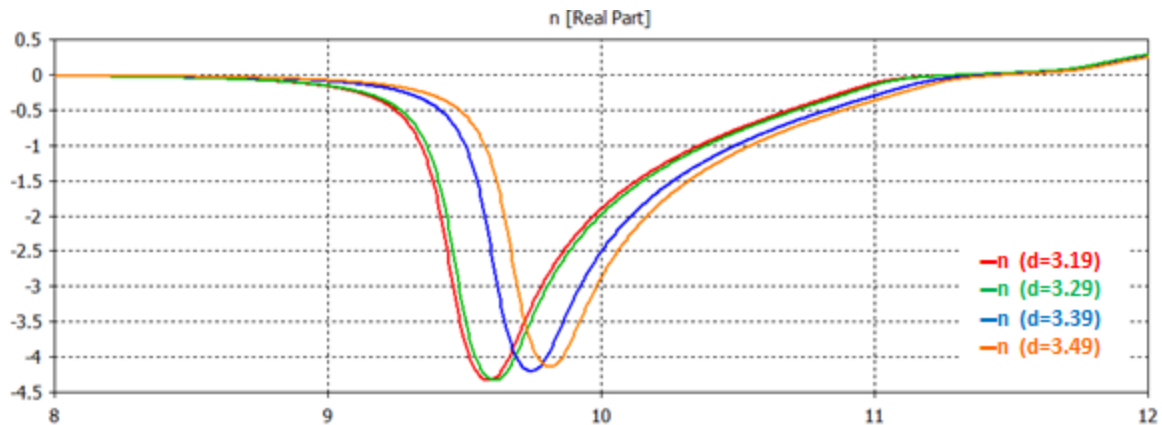


Figure 16. Real part of refractive index for different area between two the rings as in (sq- sq) design.

Effect of metal width (wt):

Here, the width of metal were changed of both outer and inner rings, while the other parameters are kept constant ($g= 0.1$, $s= 0.14$, $a1=2.4808$, and $r1=1.4$) mm. When the metal width has been changed the area between the rings is kept constant. For the (sq- sq) and (c- sq) designs the metal width has been changed by changing the four sides length of the inner square ($a2$). While for the (c- c) and (sq- c) designs the metal width has been changed by changing the radii of the inner circle $r11$.

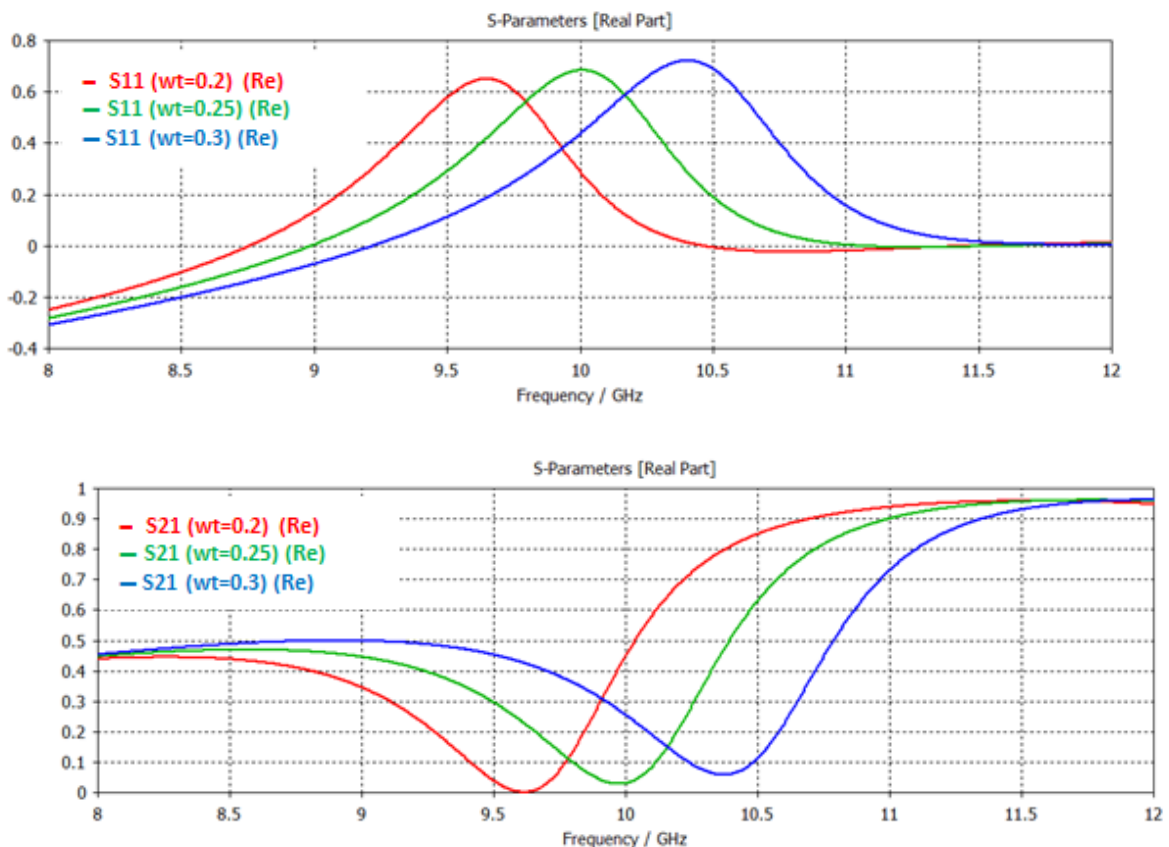


Figure 17. Real part of S11 and S21 parameters for t metal widths wt in (sq- sq) design.

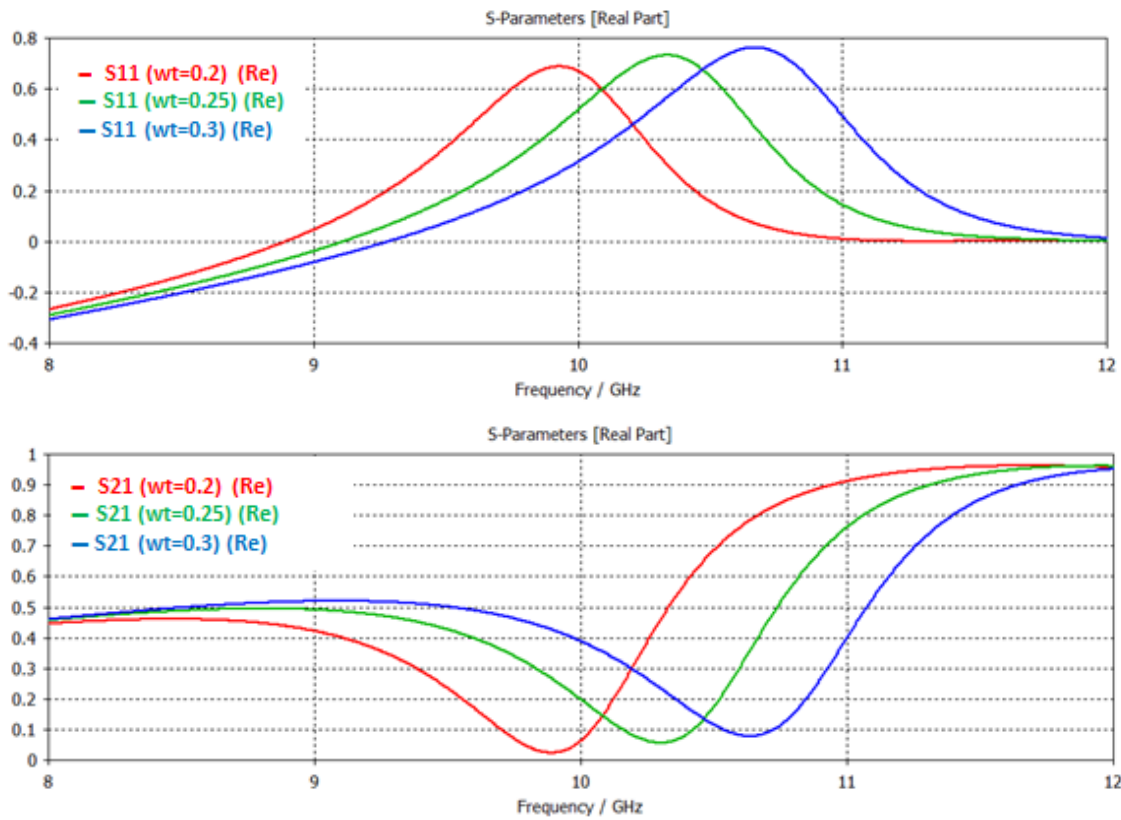


Figure 18. Real part of S11 and S21 parameters for t metal widths wt in (c- c) design.

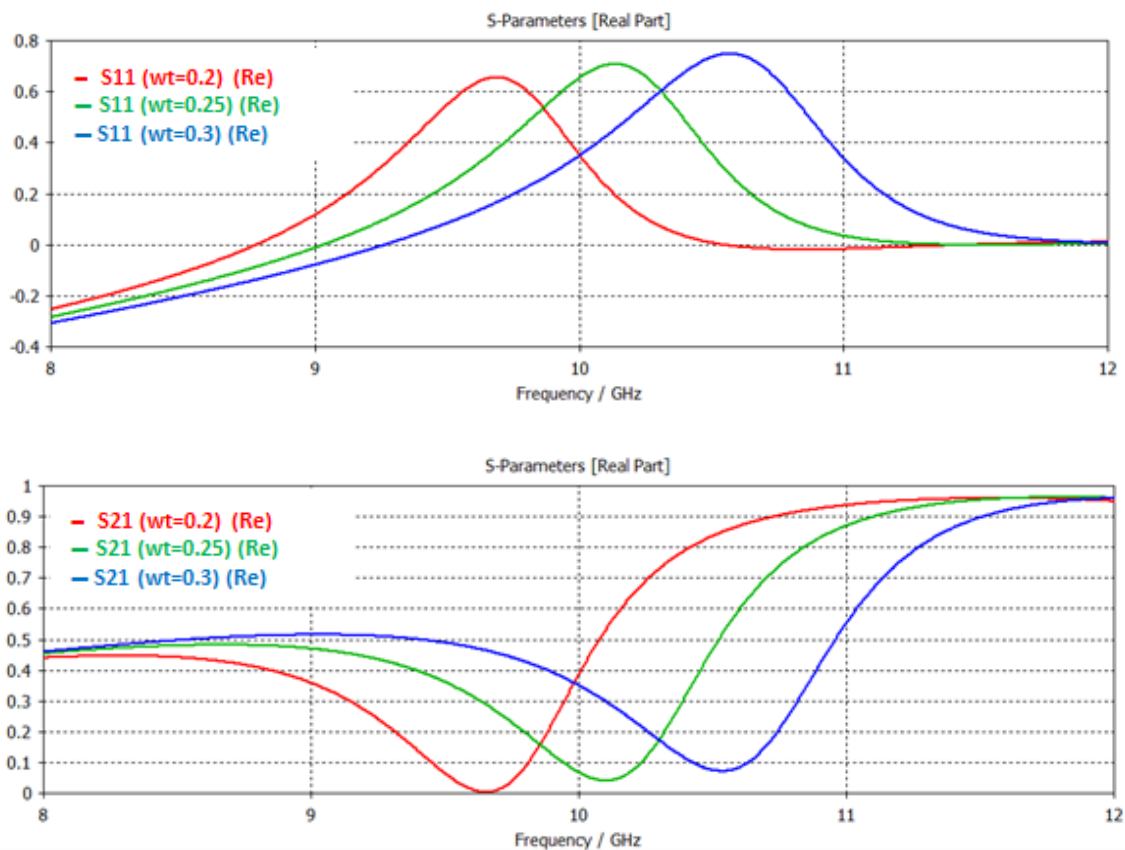


Figure 19. Real part of S11 and S21 parameters for t metal widths wt in (sq- c) design.

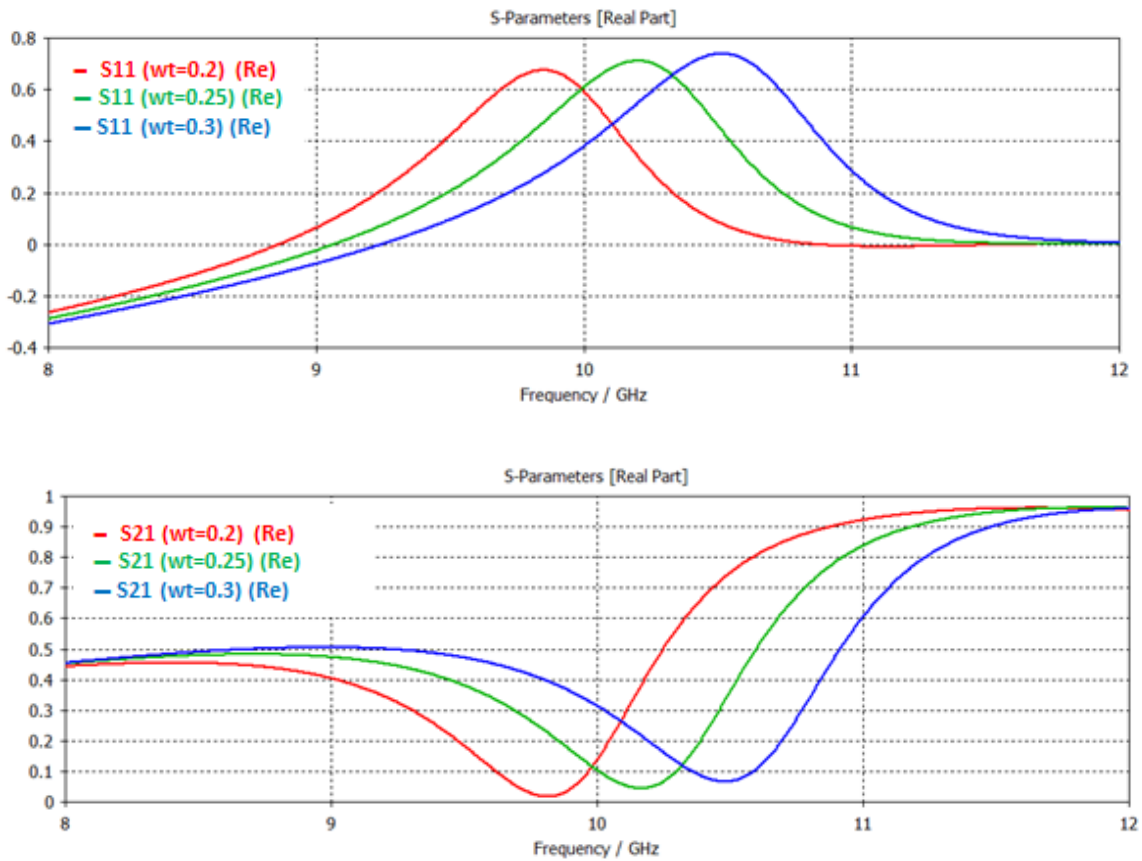


Figure 20. Real part of S11 and S21 parameters for t metal widths wt in (c- sq) design.

Table 3. Effective frequency for different metal widths.

Metal width wt (mm)	Effective frequency f (GHz)							
	For sq- sq design		For c- c design		For sq- c design		For c- sq design	
	S11real	S21real	S11real	S21real	S11real	S21real	S11real	S21real
0.2	9.638	9.62	9.928	9.91	9.688	9.682	9.848	9.832
0.25	9.81	9.78	10.336	10.32	9.9	9.88	10.2	10.18
0.3	10.33	10.31	10.668	10.662	10.404	10.392	10.516	10.5

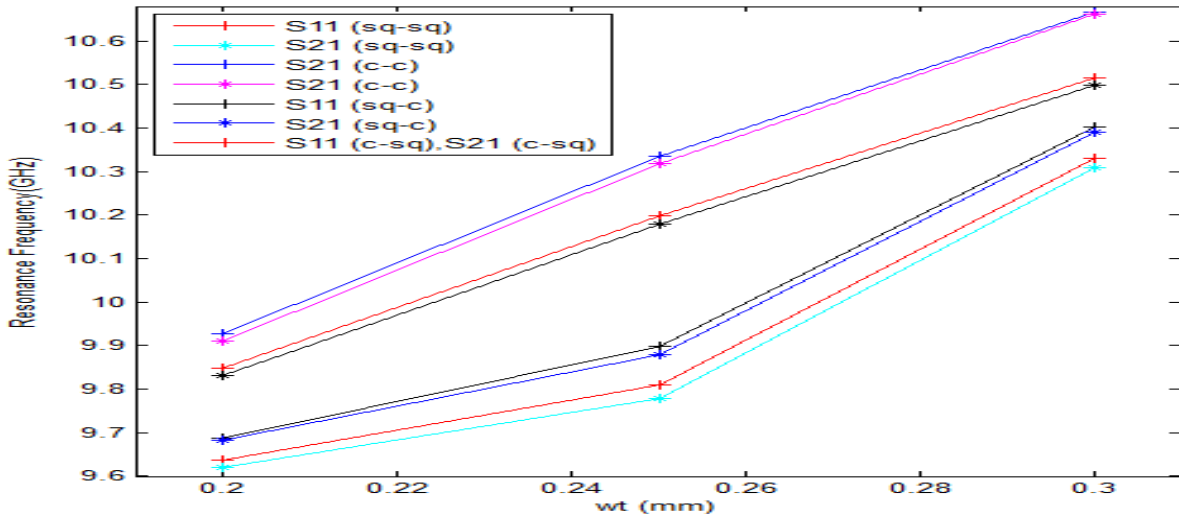


Figure 21. The values of resonance frequency versus the metal widths

When (wt) increases leads to a decrease in mutual capacitance and mutual inductance of the system. So, this will lead to an increase in ω_m , as illustrated in table 3 and Figure 17. By looking to figure 21 it can be concluded that the largest value of resonant frequency is for the design (c- c) and then (c-sq), (sq- c) and (sq-sq).

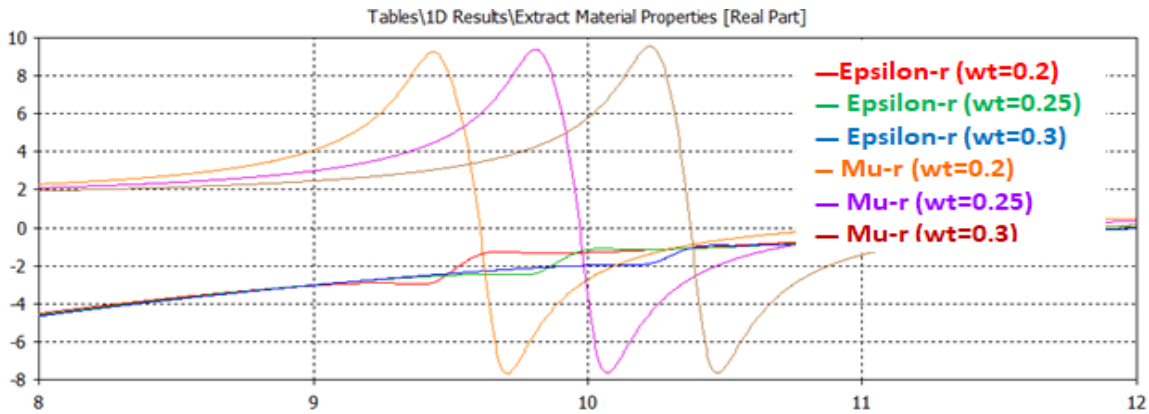


Figure 22. Real parts of electric permittivity ϵ and magnetic permeability μ for different split widths as in (sq- sq) design

From S- parameters, the real and imaginary values of ϵ_{eff} and μ_{eff} have been extracted. The real part of both ϵ_{eff} and μ_{eff} are negative about limited frequencies, as in Figure 22. Therefore $\epsilon_{eff} < 0$ and $\mu_{eff} < 0$ are simultaneously satisfied about (9.8- 12) GHz, so n_{eff} is negative values in the same frequencies as in Figure 23.

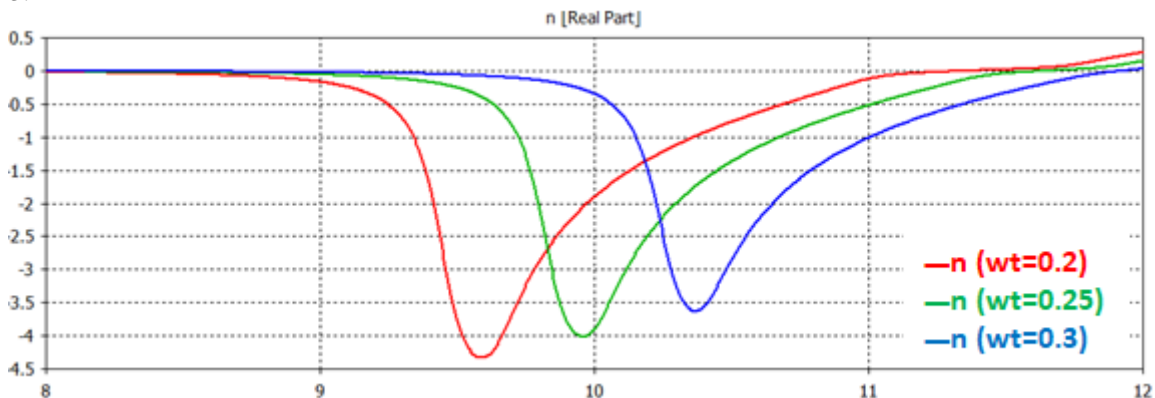


Figure 23. Real and imaginary parts of refractive index for different metal width as in (sq- sq) design.

4. Conclusions

In this work, the shape of SRR is changed to have four designs which are circle- circle, circle- square, square-circle and square- square. It found that the resonant frequency is largest for circle-circle and then circle-square, square- circle and finally square- square. It was found that the resonant frequency is also affected by changing the dimensions of SRR. When changing the width of the splits, this leads to a decrease in the capacitance between the splits because it is inversely proportional to the distance of the split, and therefore the resonant frequency increases as it is inversely proportional to the capacitance. When the area between the two rings increase, this means a decrease in the area of the inner ring and this leads to a decrease in mutual inductance and mutual capacitance where both are directly proportional to the radius of the inner ring, and this means an increase in the resonant frequency. Finally when the width of the metal increased, which is followed by a decrease of the inner ring, this also leads to an increase in the resonant frequency for the same previous reason.

Declaration of competing interest

The authors declare that they have no any known financial or non-financial competing interests in any material discussed in this paper.

Funding information

No funding was received from any financial organization to conduct this rese

5. Reference

1. K. Gangwar, Paras and R. P. S. Gangwar, "Metamaterials: Characteristics, Process and Applications", *Advance in Electronic and Electric Engineering*, 4, 1, pp. 97-106, 2014.
2. J. Zhao, "The Reliability of Split Ring Resonator Based metamaterials in Plasma Environment", Master thesis, The Pennsylvania State University, USA. 2016.
3. B. Moradi, "High dielectric permittivity materials in the development of resonators suitable for metamaterials and passive filter devices at microwave frequency," PhD thesis, Autonomous university of Barcelona, Catalonia, Spain, 2016.
4. A. T. Devapriya, S. Robinson, "Investigation on Metamaterial Antenna for Terahertz Applications", *Journal of Microwaves, Optoelectronics and Electromagnetic Applications*, vol. 18, no. 3, pp. 377-389, 2019.
5. S. D. S. Ghosh, D. Samantaray and S. Bhattacharyya, "Meander-line-based defected ground microstrip antenna slotted with split-ring resonator for terahertz range," *Engineering Reports*, vol. 2, no. 1, 2020.
6. N. A. Othman, M. A. Jamlos, W. A. Mustafa and S. Z. S. Idrus, "Simulation Study of Metamaterial Effect towards Ultra Wide Band Antenna", *International Conference on Technology, Engineering and Sciences*, 917, pp. 1-10, 2020.
7. M. T. Islam, M. Moniruzzaman, T. Alam, M. Samsuzzaman, Q. A. Razouqi and A. F. Almutairi, "Realization of frequency hopping characteristics of an epsilon negative metamaterial with high effective medium ratio for multiband microwave applications", *Scientific Reports*, vol. 11, pp. 1- 22, 2021.
8. M. Moniruzzaman, M. T. Islam, M. R. Islam, N. Misran and M. Samsuzzaman, "Coupled Ring Split Ring Resonator (CR-SRR) Based Epsilon Negative Metamaterial for Multiband Wireless Communications with High Effective Medium Ratio", *Journal Pre-proofs*, vol. 18, 2020.
9. T. A. K. Al-Musawi, S. A. Mahdi, S. Y. H. AL-Asadi, "Characteristics of Left Handed Materials", 19, 11, 1- 14, *NeuroQuantology*, 2021.
10. M. A. Hindy, R. M. ElSagheer and M. S. Yasseen, "A Circular Split Ringe Resonator (CSRR) Left Handed Metamaterial (LHM) having Simultaneous Negative Permeability and Permittivity", *International Journal of Hybrid Information Technology*, 10, 1, 171- 178, doi.org/ 10.14257/ijhit.2017.10.1.15. 2017.
11. B. M. Yao, Y. S. Gui, X. S. Chen, W. Lu and C. M. Hu, "Experimental realization of negative refraction using one metasurface", *Applied Physics Letters*, 106, 12, 121903, doi.org/10.1063/1.4916369, 2015.

12. S. T. B. Paul, "Dual band electrically small complementary double negative structure loaded metamaterial inspired circular microstrip patch antenna for WLAN applications," *Appl. Sci.*, vol. 12, no. 3035, 2022.
13. S. Zhang, Z. Wei, L. Xu, J. Xu, S. Ouyang and Y. Shen, "Plasmonic Fishnet Structures for Dual Band THz Left- Handed Metamaterials", *Photonics*, **8**, 116, 2- 7, doi.org/10.3390/photonics8040116, 2021.
14. L. S. Z. Zerrouk, "Effect of circular split ring resonator array on circular microstrip antenna used for intelligent transportation system (ITS)", *International Journal of Science and Research (IJSR)*, vol. 9, no. 6, 2020.